

Ozone, Column ClO, and PSC measurements made at the NDSC Eureka observatory (80°N, 86°W) during the spring of 1997

D.P. Donovan¹, H. Fast², Y. Makino³, J.C. Bird¹, A.I. Carswell¹, J. Davies², T.J. Duck¹, J.W. Kaminski⁴, C.T. McElroy², R.L. Mittermeier², S.R. Pal¹, V. Savastiouk⁵, D. Velkov¹, and J.A. Whiteway⁶

Abstract. During winter/spring 96/97 ozone levels over the Eureka NDSC observatory (80°N,86°W) were measured using a lidar, sondes, and a Brewer spectrophotometer. Column ClO measurements were also made using an FTIR system. Measurements show that lower stratospheric ozone mixing ratios decreased rapidly between mid-February and late-March though the ozone mixing ratio losses appear to have been less than for the 95/96 season. Elevated column amounts of ClO were found to be present over Eureka until late March.

Introduction

In recent years, springtime losses in Arctic lower stratospheric ozone have been observed. Although not as marked as the declines observed in Antarctic ozone levels, the reductions in Arctic lower stratospheric ozone amounts have been substantial [Müller *et al.*, 1996; Manney *et al.*, 1996; Donovan *et al.*, 1996]. It appears that for large scale ozone loss to occur, stratospheric chlorine compounds must be converted from inert reservoir forms into active forms (chlorine activation). In the presence of sunlight, these active chlorine compounds will engage in catalytic ozone destruction. Enhanced levels of ClO are indicative of this process [Salawitch *et al.*, 1993].

Chlorine activation is believed to occur via heterogeneous chemical reactions on stratospheric HNO₃/H₂O/H₂SO₄ aerosols (with various fractional compositions and phases) at temperatures below around 195 K [Kawa *et al.*, 1997]. At temperatures approaching 195 K, heterogeneous reaction probabilities associated with the "background" mainly sulphate/water aerosol greatly increase, leading to significant chlorine activation [Del Negro *et al.*, 1997]. At temperatures below around 193 K, the aerosol may grow significantly via increased absorption of HNO₃ [Carslaw *et al.*, 1994] leading to polar stratospheric cloud (PSC) formation. PSCs not only engage in chlorine activation, but they also provide a means whereby

nitrogen oxide species (NO_x) which deactivate active chlorine (and hence limit the amount of ozone loss) may be sequestered (or removed via sedimentation) from the gas phase.

Compared to the southern hemisphere (SH) polar vortex, the northern hemisphere (NH) vortex is generally warmer and not so long-lived [Schoeberl and Hartmann, 1991]. Comparable amounts of chlorine activation in both hemispheres have been observed [Pfeilsticker *et al.*, 1997]. However, since the amount of ozone loss also depends on the amount of sunlight the processed air receives and the degree to which sequestering/removal of gas phase NO_x has been achieved, there is generally less stratospheric ozone loss in the Arctic than in the Antarctic. For similar reasons, the large year-to-year variation of the strength of the NH vortex leads to large yearly variations in the degree of Arctic ozone depletion [Müller *et al.*, 1996]. In terms of the behavior of the NH polar vortex, the last two seasons have been highly unusual. The 95/96 vortex was stronger and colder than normal for much of the winter while for 96/97 the early vortex was weaker and warmer than usual. However, in February 97, minimum lower stratospheric vortex temperatures fell well below 195K (the approximate threshold for chlorine activation) and the vortex remained cold and well-established much later into the spring than is usual [Coy *et al.*, 1997; Santee, *et al.*, 1997].

From late November 1996 to March 18, 1997 the AES/ISTS ozone differential absorption lidar (DIAL) system was operated at the NDSC (Network for Detection for Stratospheric Change) observatory at Eureka (80°N, 86°W). The system is used to make stratospheric ozone, aerosol, and temperature measurements. It is a nighttime only system and is described elsewhere [Donovan *et al.*, 1995]. In addition, numerous ECC ozone sondes (as well as twice daily standard meteorological sondes) were launched from Eureka throughout the season. With returning sunlight, ozone column measurements were conducted using a Brewer spectrophotometer from early March onwards. Numerous infrared solar absorption spectra were also acquired using a Fourier transform spectrometer system from mid-February well into April. These spectra can be analysed to yield column amounts of various species. However, for this season only column ClO amounts for a few days have been derived to date.

Ozone Measurements

The lidar and ECC sonde ozone measurements made at Eureka from December 1, 1996 to April 15, 1997 are shown in Figure 1 along with with potential vorticity (PV) calculated from the Canadian Meteorology Center (CMC) analysis. The data shown are averaged for four different isentropic θ levels. When both ozonesonde and lidar ozone measurements are available the ozone mixing ratios generally agree within under

¹ISTS/York U. Dept. of Physics and Astronomy, North York, ON., Canada.

²Atmospheric Environment Service (AES), North York, ON., Canada.

³Meteorological Research Institute (MRI) Tsukuba, Japan.

⁴York University, Dept. of Earth and Atmospheric Science (EATS).

⁵York University, Dept. of Physics and Astronomy. North York, ON. Canada.

⁶University of Toronto, Dept. of Physics, Toronto, ON., Canada.

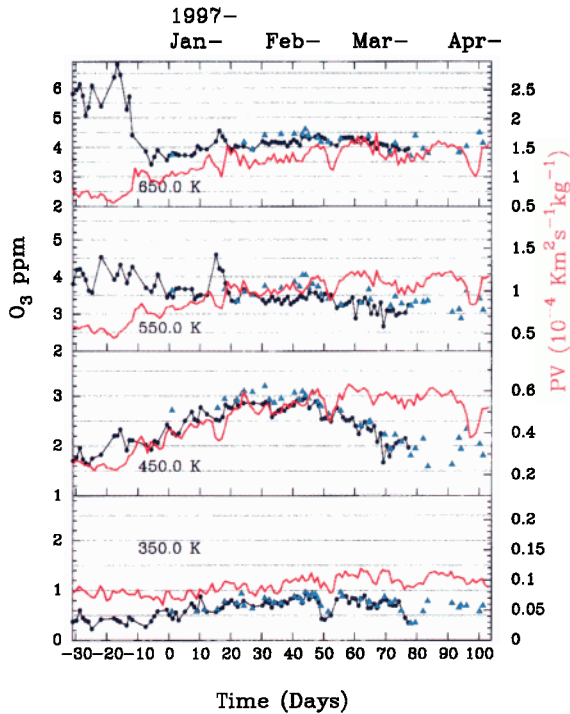


Figure 1. Lidar derived ozone mixing ratio (dark blue), ozone sonde measurements (light blue triangles) and CMC potential vorticity (red) for different potential temperature levels. The values shown are averages over ± 50 K about the θ levels shown.

0.1ppm. Figure 1 shows that around the the 450 K level, ozone mixing ratios reached a maximum of around 3 ppm in early February and then decreased to a minimum of about 1.6-1.8 ppm in late March.

To distinguish between periods when the Eureka was inside from periods when Eureka was outside of the vortex, the ozone measurements were compared both to PV and the observed lidar aerosol scattering ratio, R , (ratio of the total aerosol and molecular backscattering to the molecular backscattering alone). Due to the existence of the transport barrier associated with the vortex edge and the occurrence of strong diabatic descent within the vortex the amount of background aerosol within the vortex is much lower compared to that of mid-latitude air at the same level [Dameris *et al.*, 1995]. From mid-January until the end of March, low background scattering ratios above 450 K (not shown) and PV within about 85% of the vortex maximum indicate that the lower stratosphere above Eureka was within the confines of the vortex. The increase in ozone mixing ratios in early April occurred as the vortex center, where ozone loss tended to be stronger [Manney *et al.*, 1997], moved further from Eureka.

The average intra-vortex ozone mixing ratios measured for the 95/96 and 96/97 seasons as a function of potential temperature are shown in Figure 2. Only measurements which were considered to be inside the confines of the vortex between 450 and 600 K were included in the averages. Lidar data were used for all the profiles shown except for the March 16-April 2 profile which was constructed using ozonesonde data. The large variability present in the average ozonesonde profile above 600 K is due to the few sondes that reached

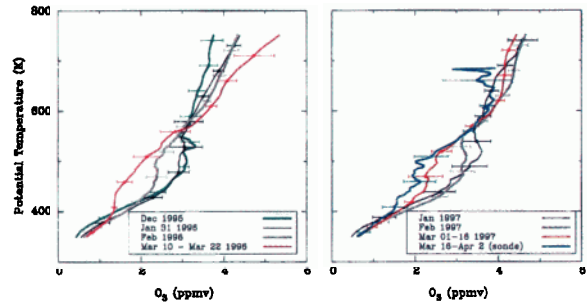


Figure 2. Average intra-vortex ozone mixing ratio profiles throughout the 95/96 (left) and 96/97 (right) measurement periods. The error bars show the standard deviation of the mean profiles.

this altitude. The Eureka lidar measurements agree well with average intra-vortex MLS ozone measurements made in February [Manney *et al.*, 1997] and with HALO measurements made in March [Müller *et al.*, 1997].

In general, in any given season, the occurrence of strong diabatic descent associated with the vortex may be expected to increase lower stratospheric ozone levels by transporting ozone rich air downward. For the 95/96 above 550 K a smooth increase in ozone mixing ratios with time is seen. Such a trend is consistent with the occurrence of strong regular diabatic descent [Browell *et al.*, 1993]. For 96/97 such a trend does not clearly seem to be present pointing to differences in transport between the two years.

Consistent with chemical ozone loss, below about 550 K there is a decrease in the observed intra-vortex ozone mixing ratios. For 96/97 mid-March lower stratospheric ozone mixing ratios are higher (about 2.1 ppm at 450 K) when compared to 95/96 (about 1.6 ppm at 450 K). For 95/96 a loss (including an estimate of diabatic descent effects) on the order of 50 % (1.1-1.3 % per day) between mid-January and mid-March was inferred [Donovan *et al.*, 1996]. This compares to a loss of 30-35 % (1.7-1.8 % per day) between mid-February and late-March 97. No account of transport effects were taken into account for the 97 estimate.

Column Ozone

Figure 3 shows the total ozone measured over Eureka using sondes, lidar, and a Brewer from early December to late April. The lidar column measurements were inferred by assuming a constant ozone mixing ratio (0.02-0.04 ppm) below the minimum lidar measurement altitude (7km). The Brewer derived column amounts include results from the commonly used solar measurements in the ultra-violet as well as preliminary results from a newly developed solar absorption method that uses the Chappuis band of ozone near 600 nm [V. Savastiouk *et al.*, in preparation, 1997]. This new method extends the range of total ozone measurements to sun angles as low as 4 degrees.

In Figure 3 only sondes that reached above 20 mb have been used. The lidar and Brewer results both agree well with the column amounts measured by ozone sondes. The measurements show that column ozone amounts generally decreased from mid-January onwards until early April. Column ozone amounts fell below 300 DU in early March and a minimum of around 220 DU was reached for a very short duration

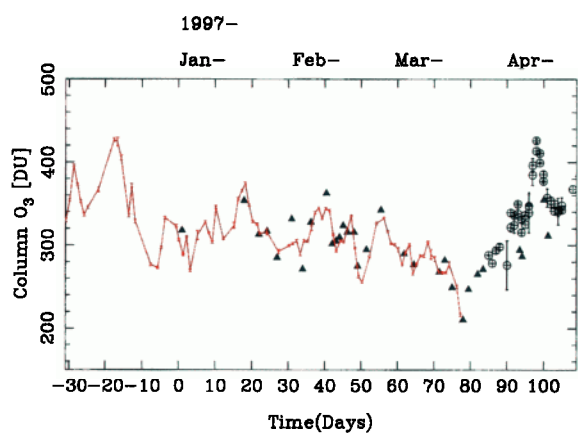


Figure 3. Integrated ozone over Eureka. Results from ozonesondes (blue triangles) Brewer measurements (black crossed circles) and lidar measurements (red) are shown.

around March 18-19. This minimum value is around the NH column minimum measured by the TOMS instrument at this time [Neuman *et al.*, 1997]. The very low March 18-19 column amounts were associated with the passage of an upper tropospheric anti-cyclone [McKenna *et al.*, 1989].

PSC Observations

From early February onwards temperatures above Eureka at the $\theta = 400$ -500 K levels often approached or fell below 195 K (the NAT existence temperature), however, significant enhancements in the lidar backscatter profiles were noted only when the temperature fell below around 193 K. This suggests that the PSCs observed this season over Eureka were type Ib PSCs (i.e. liquid $\text{HNO}_3/\text{H}_2\text{O}/\text{H}_2\text{SO}_4$) droplets that grow significantly at temperatures below about 193 K [Carslaw *et al.*, 1994]. This observation is consistent with other previous findings [Dye *et al.*, 1996].

For the 96/97 season PSCs were observed as late as March 18 (after which time the lidar was shut down due to increasing sunlight). This is much later in the season than PSCs have ever been previously observed over Eureka. Figure 4 shows a sequence of aerosol scattering ratio profiles along with the corresponding temperature profiles for March 14-19. The presence of PSCs associated with low temperatures is clearly seen between about 15 and 20 km for the March 18 and March 19 profiles. The temperature profiles shown are a combination of sonde measurements and lidar derived temperatures. Below about 25 km the lidar temperatures were derived using a modified form of the well known Rayleigh technique applied to the Raman N_2 lidar backscatter signals at 385 nm, this was done to avoid the errors associated with additional elastic backscatter from the aerosols [Evans *et al.*, 1997]. The temperatures derived in this way agreed with the sonde measurements within about 0.5K in the lower stratosphere.

Column ClO measurements

Solar transmission spectra were recorded at 0.004 cm^{-1} resolution with a Bomem DA8 Fourier transform spectrometer system, from late February until late April. The ClO column measurements presented in this paper are based on

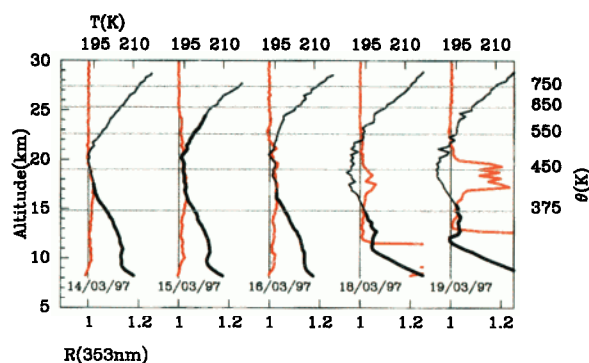


Figure 4. Scattering ratio (R) profiles in red along with the lidar derived temperature profile (blue) and sonde temperature profile (black). The vertical line denotes $R=1$ and $T=193 \text{ K}$. The large increases in R near the tropopause for the 18-19th are caused by the presence of cirrus clouds.

the P(8.5), P(10.5) and P(11.5) absorption features in the (0-1) vibration-rotation band of Cl^{35}O . The columns were derived using a non-linear least-squares spectral fitting algorithm applied to narrow spectral windows containing the ClO absorption features. An a priori profile consisting of a constant mixing ratio of 2.5 ppbv in a six-km thick layer centered over the observed PSC altitude range, and essentially no ClO elsewhere was employed. A good fit to the ClO line shapes was achieved, an example of which appears in Figure 5. Changing the a priori ClO profile in altitude by one or two kms or reducing the layer thickness down to 2 km had no significant effect on the fit and changed the derived column amounts by only a few percent.

The column amounts derived from the individual spectra were averaged for each day of observation. These daily means are plotted in Figure 6 as a function of time. The error bars represent the standard deviations of the individual measurements of which there are typically 9 or 12 each day (i.e. 3 spectra \times 3 lines). The measured ClO columns are consistent with layer-average mixing ratios decreasing from approximately 1.6 ppbv on February 27 to 0.7 ppbv by March 20 in the 14-22 km altitude region. The MLS instrument on UARS measured elevated levels of ClO when viewing the NH in late January, and from mid-February to early March [Santee, *et al.*, 1997]. The FTIR measurements made in late February are consistent with the vortex average values measured by the MLS at this time. By April 10th when MLS ClO measurements were again made, they showed very little ClO. The FTIR measurements indicate that elevated levels of ClO were present in the stratosphere over Eureka until the vortex moved away from Eureka around March 20th.

Summary

The 96/97 ozone and ClO measurements made at Eureka are consistent with the occurrence of substantial chemical depletion. The Eureka measurements are consistent with the vortex-average results from the MLS and HALOE instruments. The Eureka measurements are limited in the sense that they represent only one ground station. However, compared to the HALOE and MLS measurements which only sampled the vortex for limited time periods, the lidar and sonde measurements of ozone represent a near continuous

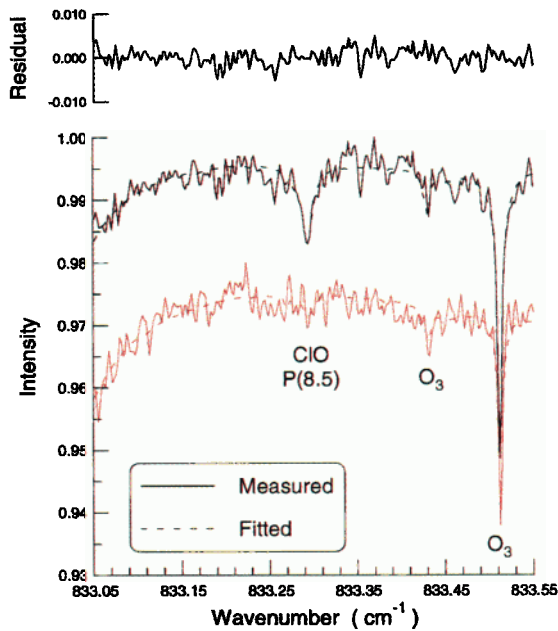


Figure 5. The spectral fit obtained in the region of the P(8.5) ClO line recorded on 27 February, 1997, at a solar zenith angle of 88.8 degrees. The residuals for this fit are plotted immediately above. In red and shifted down, the spectrum recorded on 20 March, 1997 is shown for comparison.

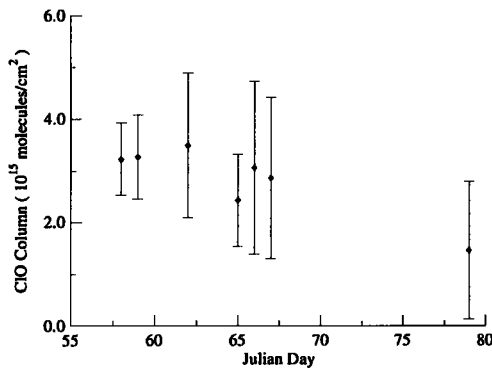


Figure 6. Daily mean ClO column amounts observed over Eureka after polar sunrise in 1997.

height-resolved data set.

Rapid ozone loss was seen to occur over Eureka from mid-February until late March. However, for the 96/97 season, compared to 95/96, intra-vortex lower stratospheric ozone mixing ratios over Eureka were generally higher. This tends to support the claim that while significant chemical depletion of Arctic ozone occurred within the polar vortex, direct dynamical effects must have played a key role in bringing Arctic column ozone to the low levels reached during March 97 [Fioletov et al., 1997; Newman et al., 1997].

Acknowledgments. Financial and technical support was provided by ISTS and by AES. The technical support of the CMC and financial support of the Science and Technology agency of Japan is also gratefully acknowledged.

References

- Browell, E.V. et al., Ozone and aerosol changes during the 1991-92 airborne Arctic stratospheric expedition, *Science*, **261**, 1155-1158, 1993.
- Carslaw, K.S. et al., Stratospheric aerosol growth and HNO₃ gas phase depletion from coupled HNO₃ and water uptake by liquid particles, *Geophys. Res. Letts.*, **23**, 2479-2482, 1994.
- Coy L., E.R. Nash, and P.A. Newman, Meteorology of the Polar Vortex: March 1997, *Geophys. Res. Letts.*, *this issue*.
- Dameris M., M. Wirth, W. Renger and V. Grewe, Definition of the Polar Vortex Edge by Lidar data of the stratospheric Aerosol: A Comparison with Values of Potential Vorticity, *Beitr. Phys. Atmosph.*, **68**, 113-119, 1995.
- Del Negro L.A., Evaluating the role of NAT, NAD, and liquid H₂SO₄/H₂O/HNO₃ solutions in Antarctic polar stratospheric cloud aerosol: Observations and implications, *J. Geophys. Res.*, **102**, 13225-13282, 1997.
- Donovan, D.P., J.C. Bird, J.A. Whiteway, T.J. Duck, S.R. Pal, and A.I. Carswell, Lidar Observations of Stratospheric Ozone and Aerosol above the Canadian High Arctic During the 1994-95 Winter, *Geophys. Res. Letts.*, **22**, 3489-3492, 1995.
- Donovan, D.P., J.C. Bird, J.A. Whiteway, T.J. Duck, S.R. Pal, A.I. Carswell, J.W. Sandilands, and J.W. Kaminski, Ozone and aerosol observed by Lidar in the Canadian Arctic during the winter of 1995/96, *Geophys. Res. Letts.* **23**, 3317-3320, 1996.
- Dye J.E. et al., In-situ Observations of an Antarctic Polar Stratospheric Cloud: Similarities with Arctic Observations, *Geophys. Res. Letts.*, **23**, 1913-1916, 1996.
- Evans K.D., S.H. Melfi, R.A. Ferrare, and D.N. Whiteman, Upper tropospheric temperature measurements with the use of a Raman lidar, *Appl. Opt.*, **36**, 2594-2602, 1997.
- Fioletov V.E., J.B. Kerr, D.I. Wardel, J. David, E.W. Hare, C.T. McElroy, D.W. Tarasick, Long-term decline of ozone over the Canadian Arctic until early 1997 from ground-based and balloon sonde measurements, *Geophys. Res. Letts.*, *this issue*
- Kawa S.R., et al., Activation of chlorine in sulfate aerosol as inferred from aircraft observations, *J. Geophys. Res.*, **102**, 3921-3933, 1997.
- Manney, G.L., M.L. Santee, L. Froidevaux, J.W. Waters, and R.W. Zurek, Polar vortex conditions during the 1995-96 Arctic winter: Meteorology and MLS ozone, *Geophys. Res. Letts.*, **23**, 3203-3206, 1996.
- Manney, G.L., L. Froidevaux, M.L. Santee, R.W. Zurek and J.W. Waters, MLS observations of Arctic ozone loss 1996-97, *Geophys. Res. Letts.*, *this issue*, 1997.
- McKenna D.S., R.L. Jones, J. Austin, E.V. Browell, M.P. McCormick, A.J. Krueger and A.F. Tuck, *J. Geophys. Res.*, **94**, 11641-11668, 1989.
- Müller R., P.J. Crutzen, J-U. Grooß, C. Brühl, J.M. Russell and A.F. Tuck, Chlorine activation and ozone depletion in the Arctic vortex: Observations by the Halogen Occultation Experiment on the Upper Atmosphere Research Satellite, *J. Geophys. Res.* **101**, 12531-12554, 1996.
- Müller R., Jens-Uwe Grooß, D.S. McKenna, P.J. Crutzen, C. Brühl, J.M. Russell, and A.F. Tuck, *Geophys. Res. Letts.*, *this issue*, 1997.
- Newman, P.A., J.F. Gleason, and R.S. Stolarski, Anomalously low ozone over the arctic, *Geophys. Res. Letts.* *this issue*, 1997
- K. Pfeilsticker et al. Aircraft-borne detection of stratospheric column amounts of O₃, NO₂, OClO, ClNO₃, and aerosols around the arctic vortex (79°N to 39°N) during spring 1993, *J. Geophys. Res.*, **102**, 10801-10814, 1997.
- Salawitch et al., Chemical Loss of Ozone in the Arctic Polar Vortex in the winter 1991-1992, *Science*, **261**, 1146-1149, 1993.
- Santee, M.L., G.L. Manney, L. Froidevaux, R.W. Zurek, and J.W. Waters, MLS observations of ClO and HNO₃ in the 1996-97 Arctic polar vortex, *Geophys. Res. Letts.* *this issue*, 1997.
- Schoeberl, M.R., and D.L. Hartmann, The dynamics of the stratospheric polar vortex and its relation to springtime ozone depletions, *Science*, **251**, 46-52, 1991.

D.P. Donovan, ISTS, 4850 Keele St., North York, ON, Canada, M3J 3K1. (e-mail: donovan@lidar.ists.ca)

(Received May 9, 1997; revised September 16, 1997; accepted October 7, 1997.)